Am J Cardiovasc Dis 2026;16(3):125-141
www.AJCD.us /ISSN:2160-200X/AJCD0171024

Original Article

Cardioprotective effect of acupuncture in mice with diabetic cardiomyopathy by alleviating cardiac fibrosis and apoptosis

Hao Hong[1,2], Lu You[1], Xin Cao[3], Jing-Han Yuan[1], Hao Li[1], Bing-Mei Zhu[1]

[1]*Regenerative Medicine Research Center, West China Hospital, Sichuan University, Keyuan Road 4, Gaopeng Street, Chengdu 610041, Sichuan, P. R. China;* [2]*The Fourth Affiliated Hospital of Soochow University, Chongwen Road 9, Suzhou 215000, Jiangsu, P. R. China;* [3]*Acupuncture and Tuina School/Third Teaching Hospital, Chengdu University of Traditional Chinese Medicine, Shierqiao Road 37, Chengdu 610075, Sichuan, P. R. China*

Received December 25, 2025; Accepted April 21, 2026; Epub June 15, 2026; Published June 30, 2026

Abstract: Objectives: The purpose of this study is to assess the effects of acupuncture on glucose control, lipid metabolism, myocardial fibrosis, and the development of diabetic cardiomyopathy (DCM) in mice with type 2 diabetes. Methods: After modelling, mice were divided into three groups: the control, model (DCM), and PC6+ST36 group. Acupuncture was applied at PC6 and ST36 acupoints for 15 min every other day, three times a week for 8 weeks during the development of diabetic cardiomyopathy. Heart function was assessed by echocardiography and electrocardiogram. Serum glucose, lipid metabolism and ANP were assessed via ELISA. The myocardium was assessed by histology, immunoblotting, RNA-seq and CUT&Tag on the day after all the treatments were finished. Results: Acupuncture at Neiguan and Zusanli reduced abnormal glucose (mean difference of fed glucose decrease from 19.63 mmol/L to 12.62 mmol/L, *P*=0.008) and improved lipid metabolism (mean difference of TC decrease from 23.70 mmol/L to 17.81 mmol/L, *P* value is 0.038, TG from 27.14 mmol/L to 18.70 mmol/L, *P* value is 0.006, LDL from 19.36 mmol/L to 14.35 mmol/L, *P* value is 0.015, FFA from 578.96 mmol/L to 328.98 mmol/L, *P* value is 0.0001) in mice with diabetic cardiomyopathy. Both impaired systolic function (mean difference of EF increase from 52.84% to 71.10%, *P* value is 0.004, FS increase from 26.39% to 39.38%, *P* value is 0.008) and damaged diastolic function (mean difference of IVRT decrease from 26.50 ms to 16.33 ms, *P* value is 0.025, E/A ratio increase from 0.91 to 1.22, *P* value is 0.07) were observed in the DCM group, whereas acupuncture enhanced cardiac function in mice with DCM. Cardiac fibrosis was alleviated in the PC6+ST36 group, accompanied by reduced expression of fibrosis-related genes (*Col1a1* family). Moreover, acupuncture inhibited cardiac apoptosis in mice with DCM to some extent. Conclusions: Acupuncture at Neiguan and Zusanli can improve heart function and myocardial hypertrophy by inhibiting cardiac apoptosis and fibrosis in mice with DCM.

Keywords: Acupuncture, diabetic cardiomyopathy, heart function, apoptosis, fibrosis

Introduction

Clinically, diabetic cardiomyopathy (DCM) is defined as obvious cardiac dysfunction in the absence of notable coronary artery disease, valvular disease and cardiovascular risk factors, which is closely related to the high incidence of heart failure and high mortality in diabetic patients [1]. Studies have shown that people with diabetes are two to four times more likely to develop cardiovascular complications and heart failure than those without diabetes [2].

Clinical DCM display impaired diastolic function in the early period, scathing systolic function in the late period, and eventually heart failure [3]. Clinical studies have shown that nonpharmacological interventions and lifestyle changes (control of body mass, smoking cessation, and aerobic exercise) can effectively alleviate cardiac remodelling in DCM patients. At present, Western medicine still lacks specific therapeutic drugs and mainly adopts symptomatic treatments, such as hypoglycemic and lipid regulation, which can only delay the progression of DCM. However, single hypoglycemic or lipid-low-

https://doi.org/10.62347/GLQJ4263

ering drugs cannot significantly reduce the incidence of cardiovascular adverse events, and there is still no single drug that can treat heart failure with preserved ejection fraction (HFpEF) in DCM. There are only two major classes of drugs: sodium-dependent glucose cotransporter-2 (SGLT-2) inhibitors [4] and glucagon-like peptide 1 receptor (GLP-1R) agonists, which may directly reduce myocardial stiffness and antifibrosis, improve myocardial energy metabolism, and thereby ameliorate cardiac diastolic dysfunction [5]. Although these drugs can significantly reduce the probability of adverse cardiovascular events, obvious side effects have hindered their promotion and application.

Many animal studies have shown that acupuncture can increase insulin sensitivity, reduce blood sugar [6] and improve abnormal lipid metabolism [7]. Our previous research revealed that acupuncture has a good lipid-lowering effect and can reverse abnormal gene expression profiles [8, 9]. The combination of electroacupuncture and rosiglitazone has a synergistic effect in the treatment of type 2 diabetes (T2DM), not only by increasing insulin sensitivity and reducing lipid accumulation but also by effectively preventing rosiglitazone-induced weight gain [10]. EA Weiwanxiashu (EX-B 3) significantly increased model rats' pancreas GLP-1R, and GLUT4 of skeletal muscle membrane; the therapy significantly decreased model rats' skeletal muscle GLP-1R, restored pancreas morphology, and reduced fasting blood glucose and insulin resistance indices [11]. The latest study by Chen Huan et al. confirmed that electroacupuncture can promote cardiac contractile function and directly prevent and treat myocardial hypertrophy and fibrosis in db/db mice [12]. Wang et al. observed the therapeutic effect of acupuncture on diabetic cardiomyopathy model rats. After 12 weeks of treatment at the Fei-Shu (BL13), Pi-Shu (BL20), Shen-Shu (BL23), Sanyinjiao (SP6), Neiguan (PC6) and Weiwan-Xia-Shu (EX-B3) points, adiponectin levels were elevated in the rats, and the myocardial fiber arrangement was slightly disordered, with no widening gap in the acupuncture treatment group, which was significantly better than that in the model group. These results indicate that acupuncture has a therapeutic effect on rats with diabetic cardiomyopathy, possibly by lowering blood glucose, increasing adiponectin expression, downregulating TNF-α expression, and normalizing myocardial structure [13, 14]. Gong et al. verified that EA at Zusanli (ST36) reduces HFD-induced hepatic lipid accumulation in male Sprague-Dawley rats through the AMPK signalling pathway [7]. Recently, another animal study demonstrated that electroacupuncture can promote lipid metabolic reprogramming in chronic heart failure model rats through cardiac glial cell modulation combined with digilanid C mediated by IL-6 [15].

Clinical evidence has also shown that electroacupuncture is an effective intervention for the treatment of insulin drug resistance [16] and diabetic complications such as diabetic peripheral neuropathy [17] and diabetic gastroparesis [18]. One of our clinical studies also confirmed the effect of electroacupuncture combined with metformin in T2DM patients compared with metformin alone, revealing that electroacupuncture significantly weight-loss effect; fasting glucose and insulin levels; the HOMA-IR index; and the levels of TNF-α, leptin and adiponectin [19].

Taken together, both animal experiments and clinical studies have confirmed that acupuncture is effective in regulating diabetic glucose and lipid metabolic abnormalities through multiple signalling pathways. Mechanistically, acupuncture focus on modulating the neuro-endocrine-immune axis and autonomic system, regulating gut microbiota, and activating insulin signaling pathways [20]. Moreover, most of these studies choose individual acupoints, while few studies have comprehensively evaluated the protective effect of acupuncture based on group acupoints in treating and delaying the progression of DCM as a complementary intervention, especially the mechanism, which is not fully understood and is an urgent problem to be solved at present.

Histone modification provides a new direction for the exploration of DCM mechanisms. As a recent research hotspot, methylation and acetylation are among the most common methods [21]. It is generally believed that the originating state enhancer is marked by the monomethylation/dimethylation of H3K4 (H3K4me1/2). Furthermore, enhancers can be activated by H3K4me1/H3K4me2 and subsequently by H3K27ace, which is catalysed by the acetylases CBP/p300 [22]. Our previous study veri-

fied that acupuncture promotes angiogenesis through H3K9 acetylation level at the *Vegf* gene after myocardial ischemia [23]. KMT2D has also been shown to play a protective role in myocardial ischemic injury in mice, and we found that KMT2D attenuates angiogenesis by inhibiting the activation of VEGF-A transcription in the ischemic heart [24], which directly methylate H3K4, in turn binding to *Rasd1* GRE motifs in its enhancers and promoting its transcription in the presence of serum [25].

According to traditional Chinese medicine theory, Neiguan can directly enhance heart function as the symptom, while Zusanli can improve lipid metabolism as the root. In this study, we aimed to elucidate the multiple protective effects of acupuncture at Neiguan and Zusanli acupoints on improving heart function (including diastolic function and systolic function) in mice with diabetic cardiomyopathy through alleviating cardiac fibrosis and reducing cardiomyocyte apoptosis. Finally, we also preliminarily explored the important role of histone modification in the ability of acupuncture to delay the progression of diabetic cardiomyopathy from a different perspective.

Materials and methods

Animals, modelling and grouping

Four-week-old C57BL/6J male mice were supplied by Ensville Biological Technology Co., Ltd. (Chengdu, Sichuan, China). The mice were housed at a constant temperature (23±1°C) under a 12/12-h light-dark cycle, with free access to food and water. All procedures were approved by the Ethics Committee for Animal Care and Use of our university (No. 20211002A), and all procedures were conducted in accordance with the guidelines of the National Institutes of Health Animal Care and Use Committee.

Ten mice were used as the control group, and the other thirty mice were subjected to modelling. Type II diabetic model was induced by a combination of high-fat diet (HFD) and medium-dose streptozotocin (S0130, Sigma-Aldrich, Shanghai, China) injection. After exposure to the respective diets for 4 weeks, all mice were injected intraperitoneally with either STZ (120 mg/kg body weight) (HFD-fed) or vehicle (0.01 mol/L citric acid, pH 4.5) (normal-fed) [10, 26]. After 72 h, we detected glucose levels in the caudal vein, and diabetic mice with non-fasting plasma glucose levels ≥ 16.67 mmol/L were chosen for further cardiac function observation. Then, twenty successfully generated mice were randomly divided into a DCM group and an acupuncture group. In the last week of experiments, the mice were evaluated cardiac functions and sacrificed by overdose anesthesia. Briefly, mice were deeply anesthetized with 5% isoflurane until the loss of pedal withdrawal reflex was confirmed. Euthanasia was then performed by cervical dislocation in accordance with the institutional animal care. Hearts were promptly excised for further experiments.

Acupoints selection and acupuncture treatment

Zusanli was selected for the studies of obesity and diabetes, while Neiguan was used for experimental research on myocardial ischemia for long time in our team [8, 27, 28]. It has also been confirmed that Neiguan combined Zusanli stimulation could improve the symptoms of diabetic cardiomyopathy in db/db mice [11]. Therefore, these two acupoints were used in this study. Acupuncture was initiated at the Neiguan (PC6) and Zusanli (ST36) acupoints bilaterally 72 h after the diabetic model was established, and treatment was applied every other day while the mice were awake with a fixed instrument for 8 weeks in total. The mice in other two groups (the DCM group and the control group) were synchronously restricted every other day for 8 weeks. Acupoints localization the standard in Experimental Acupuncturology (Lin and Wang, 1999). The location of PC6 was at a point 1.5 mm proximal to the palm crease just above the median nerve; The location of ST36 was at the anterior tibia muscle, approximately 3 mm below the knee joint. The acupuncture needles (Beijing Zhongyan Taihe Medical Instrument Co., Lot: 191526, Φ 0.18 mm) with a length of 10 mm were folded into an "L" shape by haemostatic forceps, inserted into the PC6 and ST36 acupoints, separated by approximately 5 mm, and fixed with adhesive tape. We also pressed the needles every 5 minutes to ensure that they would not fall off and to strengthen the stimulation of the acupuncture intervention. The needles were removed after 15 minutes. Water, padding and food were changed every other day after restriction and acupuncture treatment. The experimental pro-

tocol and acupoint locations are shown in Supplementary Figure 1. For euthanizing the mice in the last week of experiments, they were anesthetized with 5% isoflurane with 99.5% O_2 respectively and placed on an ice plate for tissue harvest.

Body weight and fasting blood glucose

The mice were weighed each week after they had fasted for six hours during all eight weeks. Metabolic tests were performed using standard procedures *in vivo*. For the oral glucose tolerance test (OGTT), the mice were fasted for 12 h overnight, and blood was collected from the tail vein immediately 0,15, 30, 60, 90, and 120 min after intraperitoneal injection of glucose (2 g/kg) to determine blood glucose concentrations. For a peripheral insulin sensitivity test (ITT), the mice were fasted for 4 h, and blood glucose levels were measured 0 15, 30, 60 and 90 min after intraperitoneal injection of human insulin (0.5 U/kg). Blood glucose levels were detected using an automated blood glucose glucometer (Johnson & Johnson Biological Devices Co., Ltd., China).

Echocardiography

After two months of acupuncture intervention and observation, all the mice underwent transthoracic echocardiography under 1% isoflurane anesthesia to characterize the effects of acupuncture on cardiac structure and function using a 12-MHz transducer (Vevo 3100, FUJIFILM Visual Sonics, Inc., Canada) equipped with an MX550D detector (25-55 MHz) with a wide-band frequency-fusion phase-array transducer. The heart was visualized in B mode from a long-axis view. The left ventricle (LV) ejection fraction (EF%), fractional shortening (FS%), left ventricle posterior wall thickness at diastole (LVPWd) and left ventricle anterior wall thickness at diastole (LVAWd) were calculated in M-mode. Diastolic transmitral left ventricle inflow images were acquired from apical four-chamber views using pulsed-wave Doppler to calculate early (E) and late (atrial, A) peak filling blood flow velocities and E-wave deceleration times. The E/A ratio represents the ratio of the E wave to the A wave. The sample volume was positioned at the tips of the mitral valve leaflet in the mitral valve annulus, and the ultrasound beam was parallel to the direction of blood flow to record the maximal transmitral flow velocity.

Electrocardiogram recording

Electrocardiography was performed *in vivo* at two months after intervention. All the mice were anesthetized in an induction chamber with 3% isoflurane before being carefully positioned on the electrocardiogram recording platform, while anesthesia was maintained with 1% isoflurane through a facemask. A surface lead II electrocardiogram was recorded. To reduce stress, we completed the electrode setup and system adjustment within 5 min, and recordings from the initial 5 min in all recordings were excluded from our analyses. The 5-min electrocardiogram recordings were analyzed using LabChart 8.2.3 (AD Instruments, Australia). For morphometric examination, the hearts were immediately dissected and blotted dry. Body weight was also measured and used for normalization of heart mass.

Enzyme-linked immunosorbent assays

Blood samples were obtained and centrifuged at 3500 rpm for 10 min at 4°C and stored at -80°C after the serum was separated. The serum levels of total cholesterol (TC, JM-11915M1), triglyceride (TG, JM-03100M1), GHb (JM-02442M1), low-density lipoprotein (LDL, JM-03106M1), atrial natriuretic peptide (ANP, JM-02873M1), and insulin (JM-02862M1) were measured using commercially available kits (Jiangsu Jingmei Biological Technology Co., Ltd., Nanjing, China) in accordance with the manufacturer's instructions. Free fatty acids were detected with kits from Abcam (FFA, ab65341). All the methods and procedures strictly followed the protocols of the test kits.

Histology and fibrosis analysis

The whole heart was dissected and immediately fixed with 4% paraformaldehyde to prepare serial sections (4 μm thick) of paraffin-embedded heart tissues. Briefly, the sections were dewaxed in xylene, rehydrated in descending grades of ethanol, and washed in distilled water.

For Masson's trichrome staining, kits from Beijing G-CLONE Biological Technology Co., Ltd., China (RS3960) were used. The sections were dewaxed in xylene, rehydrated in descending grades of ethanol, and washed in distilled water. Then, the sections were stained with iron

hematoxylin solution for 3 min, differentiated in acid alcohol solution, and washed with distilled water. Next, the sections were stained with Ponceau acid fuchsin for 5-10 min and rinsed with distilled water. These slides were placed in phosphomolybdic acid solution for 1-3 min and then stained with aniline blue solution for 3-6 min. The sections were differentiated in 1% glacial acetic acid and dehydrated in ethanol, followed by xylene for 5 min. Each mount was allowed to spread beneath the coverslip by covering all the tissues. Images were acquired via a microscope (NIKON ECLIPSE E100, Japan) with an image analysis system (NIKON DS-U3, Tokyo, Japan). Fibrosis was analyzed using the Image-Pro Plus 6.0 software (Media Cybernetics, Inc., MD, USA).

Immunohistochemistry

Apoptosis in heart tissue was detected via a TUNEL kit (11684817910) from Roche, which has a DAB colour developing agent (BL732A; Biosharp Technology Co., Ltd., Hefei, Anhui, China). All the methods and procedures strictly followed the protocols of the test kits as usual.

Western blot

Protein samples were extracted from the area equidistant at the papillary muscle level in cold RIPA lysis buffer (MB-030-0050, Multi-Sciences Biotech, Hangzhou, China) containing a complete protease inhibitor cocktail (11697498001, ROCHE, Switzerland) and phosphatase inhibitor (4906837001, ROCHE, Switzerland). Then samples were separated by SDS-polyacrylamide gel electrophoresis and transferred to a 0.22 μm PVDF membrane (PI88520, Millipore, USA), which was detected using specific primary antibodies (anti-COL1a, 1:1000, GB11022-3, Servicebio, Beijing, China), (anti-BCL2, 1:1000, 05-729, Sigma-Aldrich; anti-GAPDH, 1:3000, 3683, Cell Signaling Technology). Bound antibodies were detected using rabbit peroxidase-conjugated secondary antibody (Goat Anti-Rat IgG, 1:5000, 98164, Cell Signaling Technology) and visualized by enhanced chemiluminescence (RK-18-8816-31, Multi-Sciences Biotech, China) in a chemiluminescence imaging system (Chemi Scope 6100, Clinx Science Instruments, China). The band intensity was quantified by using Image J (National Institutes of Health, USA).

Transmission electron microscopy

Heart tissues were prefixed in 3% glutaraldehyde, post-fixed in 1% osmium tetroxide, dehydrated in acetone and subsequently infiltrated with a dehydrating agent and epoxy resin at ratios of 3:1, 1:1, and 1:3 and 30 to 60 min per step. The infiltrated samples were placed into moulds, irrigated with embedding solution, warmed and allowed to form polymerized embedding blocks. Ultrathin sections (~50 nm thickness) were made using an ultramicrotome. After being stained with uranyl acetate followed by lead citrate, images of the cells were acquired using a JEM-1400 PLUS transmission electron microscope (JEOL, Japan).

RNA sequence analysis

Total RNA was extracted from the hearts of the same group of mice via a Fast Pure Cell/Tissue Total RNA Isolation Kit (RC101-01, Vazyme, Nanjing, China), and the concentration of the isolated RNA was determined with a Qubit RNA BR assay (Invitrogen, Q10211, CA, USA). The RNA library was subsequently prepared according to the TruSeq RNA Sample Preparation v2 (Illumina, 15025062) protocol. A cBot Multiplex rehybridization plate and the TruSeq SBS V3 kit (Illumina, 15021668) were used for cluster generation. Sequencing was performed via the Illumina HiSeq 2500 platform (Illumina, USA). According to the generated database, differentially expressed genes were filtered by log2-fold change (FC) ≥ |±1| and FDR < 0.05, followed by GO analysis and KEGG enrichment. For specific methods, please refer to our previous studies [8, 26, 27].

CUT&Tag assays

Cleavage under targets and tagmentation assays were performed with a Hyperactive® Universal CUT&Tag Assay Kit (No. TD903, Vazyme, Nanjing, China) according to the manufacturer's instructions [29]; for details, please also see our previous study [24]. In brief, chromatin solution was added to 1 μl of MLL4 (ABE1867, Millipore, USA) and incubated overnight at 4°C with slow rotation. The ChIP assays were performed as previously described [30]. A BigWig file, which was used for the display of dense, continuous data as a graph, was generated by the bam-Coverage command in deep-

Tools (v3.3.0) software [31], during which the CPM normalization method was used. IGV (IGV: Integrative Genomics Viewer) was used for visualization. SE regions were identified via the ROSE software developed by Richard A. Young [32].

Statistical analysis

All the data are presented as the means ± SDs. A value of $P < 0.05$ was considered statistically significant. Statistical analysis was performed using GraphPad Prism 7.0 (GraphPad Software, Inc., La Jolla, CA, USA) and SPSS 20.0 software (IBM, Chicago, USA). Multiple group comparisons were made with ANOVA, followed by the Tukey HSD test for multiple comparisons. Comparisons between two groups were performed using unpaired 2-tailed Student's t test, and rank sum test was used for more than two time points.

Results

Acupuncture alleviates abnormal glucose and lipid metabolism in mice with diabetic cardiomyopathy

Body weight was lower in the DCM group (mean difference=27.6 g) than that in the control group (mean difference=22.2 g, $P < 0.05$), with a significant increase observed in the PC6+ST36 group (mean difference=24.6 g, $P < 0.05$) (**Figure 1A**). Fasting glucose levels did not significantly differ among the control, DCM, and PC6+ST36 groups (**Figure 1B**, left column, mean difference is 5.1 mmol/L, 5.1 mmol/L, 6.7 mmol/L separately, $P > 0.05$), but fed glucose level was higher in the DCM group (mean difference=19.63 mmol/L, $P < 0.001$), while acupuncture significantly reduced the glucose level (mean difference=12.62 mmol/L, $P < 0.01$) (**Figure 1B**, right column). The fasting insulin levels (**Figure 1C**) decreased (mean difference=26.29 mIU/L) and the HOMA-IR index (mean difference=26.06) (**Figure 1D**) significantly increased in the DCM group ($P < 0.001$), whereas these changes were significantly reversed in the PC6+ST36 group (mean difference is 36.44 mIU/L and 19.54 separately, $P < 0.01$).

We then measured the serum insulin and blood glucose levels in the mice fasted for 4 or 16 hours (ITT and GTT tests). We found that the mice in the DCM group presented impaired glucose tolerance and diminished insulin sensitivity ($P < 0.001$), whereas acupuncture reversed these abnormal changes (**Figure 1E** and **1F**). For lipid metabolism, we detected total cholesterol (TC), triglyceride (TG), low-density lipoprotein (LDL), free fatty acid (FFA), glycosylated hemoglobin (GHb), and atrial natriuretic peptide (ANP) levels in the serum. All these levels were elevated in the DCM group (mean difference is 23.70 mmol/L, 27.14 mmol/L, 19.36 mmol/L, 578.96 mmol/L, 74.52 ng/ml, 270.30 ng/ml separately, $P < 0.001$), but obviously decreased in the PC6+ST36 group (mean difference is 17.81 mmol/L, 18.70 mmol/L, 14.35 mmol/L, 328.98 mmol/L, 48.69 ng/ml, 184.19 ng/ml separately, $P < 0.05$) (**Figure 1G** and **1H**). These results indicate that acupuncture can alleviate abnormal glucose and lipid metabolism in mice with diabetic cardiomyopathy.

Acupuncture improves cardiac function in mice with diabetic cardiomyopathy

As DCM is associated with impaired diastolic and systolic function in the late stage and eventually leads to heart failure, we need to assess both parameters via echocardiography. Typical echocardiogram traces for the effects of acupuncture on cardiac function and structure are shown in **Figures 2A** and **3A**. Both the ejection fraction (mean EF%=52.84, $P < 0.001$) and fractional shortening rate (mean FS%=26.39%, $P < 0.05$) in the DCM group were significantly lower than those in the control group (mean difference is 74.15% and 38.52% separately), but acupuncture intervention slightly reversed the reductions in EF% (71.10%, $P < 0.001$) and FS% (39.38%, $P < 0.01$) (**Figure 2B-D**). While acupuncture can effectively reduce the left ventricular end-systolic diameter (LVID, mean difference is 1.68 mm, $P < 0.05$) and volume (ESV, mean difference is 8.80 μL, $P < 0.01$) compared with elevated data in the DCM group (mean difference is 2.24 mm and 17.47 μL separately, $P < 0.01$) (**Figure 2E**), no significant difference was detected at the diastolic end of the left ventricular posterior (LVPWd), end-diastolic diameter (LVIDd) and end-diastolic volume (EDV) among these three groups (**Figure 2F**). In terms of diastolic function, the isovolumic diastole time (IVRT) was significantly greater in the DCM group (mean difference=26.50 ms, $P < 0.01$) than that in the control group

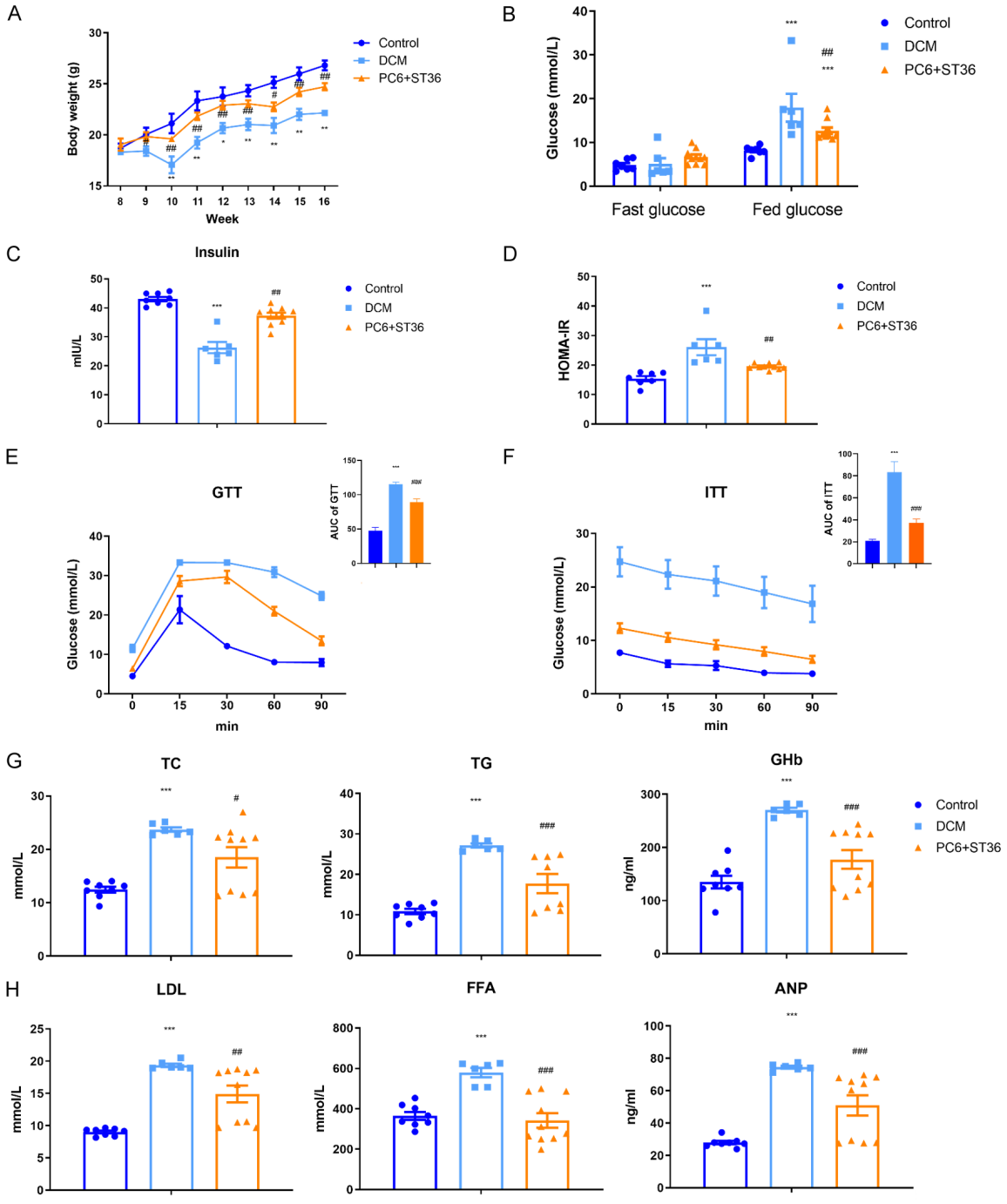

Figure 1. Acupuncture alleviates abnormal glucose and lipid metabolism in mice with diabetic cardiomyopathy. A. Observation of body weight in the control, DCM, and PC6+ST36 groups. B. Fasting and fed glucose levels were measured via a glucometer after 8 weeks of acupuncture treatment. C. Mouse serum insulin levels were determined by ELISA. D. Insulin resistance index (HOMA-IR) was calculated as (fasting insulin × fasting glucose)/22.5. E. Glucose tolerance test (GTT) after 6 weeks of acupuncture treatment. Glucose (2 g/kg) was administered i.p. after a 14 h fast (mouse age: 14 weeks). F. Insulin tolerance test (ITT) results after 8 weeks of acupuncture treatment. Insulin (0.5 U/kg) was administered i.p. after a 4 h fast (mouse age: 16 weeks). G. Serum cholesterol (TC), triglyceride (TG) and glycosylated haemoglobin (GHb) levels were measured by ELISA. H. Low-density lipoprotein (LDL), free fatty acid (FFA) and atrial brain natriuretic peptide (ANP) levels were also determined by ELISA. n=6-10 in each group. * represents $P < 0.05$, ** represents $P < 0.01$, *** represents $P < 0.001$ vs. the control group, # represents $P < 0.05$, ## represents $P < 0.01$, and ### represents $P < 0.001$ vs. the DCM group.

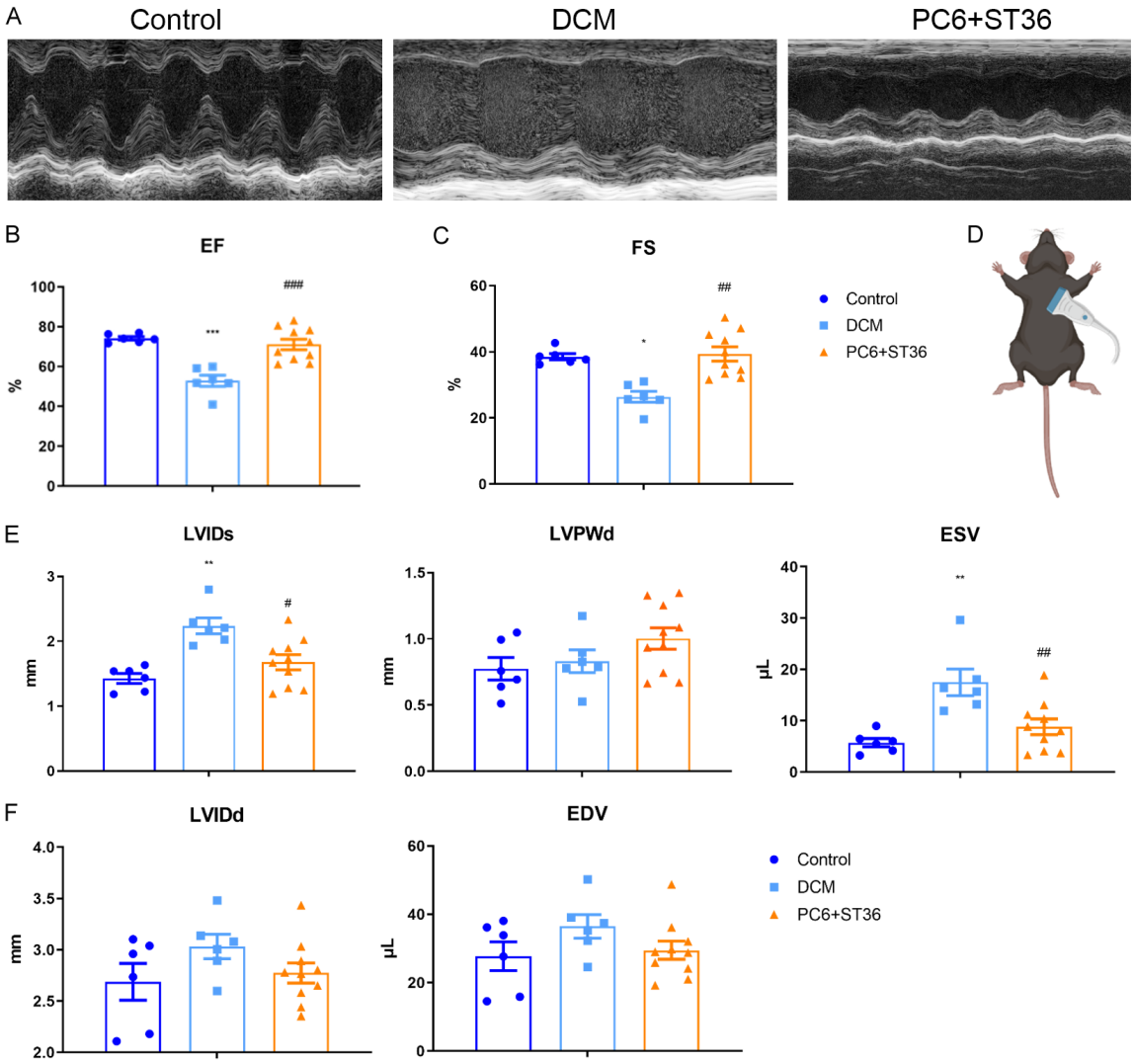

Figure 2. Cardiac systolic function in the control, DCM, and PC6+ST36 groups. A summary of echocardiographic parameters is listed below (A-F). (A) Typical echocardiogram, (B) Ejection fraction (EF), (C) Fraction shortening (FS), (D) The position of probe placement, (E) Left ventricular internal dimension systole (LVIDs), left ventricular posterior wall in diastole (LVPWd) and end-systolic volume (ESV), (F) Left ventricular internal dimension diastole (LVIDd) and end diastolic volume (EDV). n=6-10 in each group. * represents $P < 0.05$, ** represents $P < 0.01$, *** represents $P < 0.001$ vs. the control group, # represents $P < 0.05$, ## represents $P < 0.01$, and ### represents $P < 0.001$ vs. the DCM group.

(mean difference=14.11 ms), while acupuncture reduced it (mean difference=16.33 ms, $P < 0.05$). E/A ratio only showed an upward trend from 0.91 to 1.22 by acupuncture (P=0.07) (**Figure 3B**, **3C**).

The general heart weight, expressed as a ratio with body weight, was comparable among the control, DCM and PC6+ST36 groups. The ratio of heart weight/body weight tended to be lower in the PC6+ST36 group (mean difference=0.43) than that in the DCM group (mean difference=0.52, P=0.06). (**Figure 3D**, **3E**). Typical electrocardiogram traces were also recorded. Heart rate was lower than that in the DCM group (mean difference=342) compared to the control group (mean difference=423, $P < 0.05$), but acupuncture reversed this effect (mean difference=487, $P < 0.05$). A lower heart rate indicated that the vagus nerve was excited to some extent (**Figure 3F-H**). QRS interval, PR interval and T amplitude did not show obviously change.

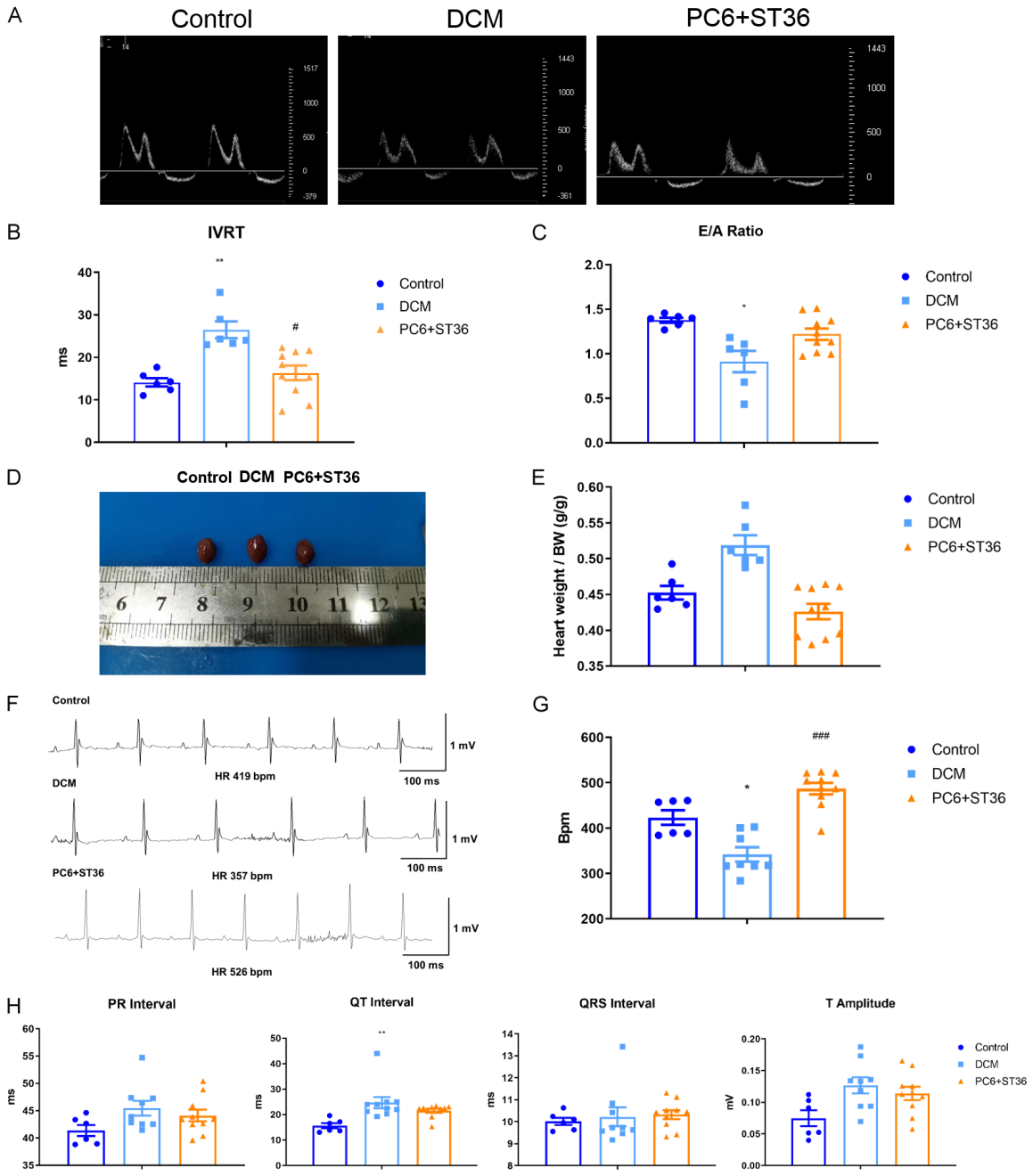

Figure 3. Cardiac diastolic function and electrophysiology in the control, DCM, and PC6+ST36 groups. A. Representative electrocardiogram of diastolic function in the control, DCM, and PC6+ST36 groups. B. Isovolumic diastole time (IVRT). C. E/A ratio (E and A represent the blood flow velocity at the early and late diastolic stages of ventricular diastole, respectively). D. Representative heart images of the three groups. E. Ratios of heart weight/body weight. F. Representative electrocardiogram recordings. G. Heart rate (HR). H. Summary of the electrophysiology data, including the PR interval, QTc, QRS width and T amplitude. n=6-10 in each group. * represents $P < 0.05$, ** represents $P < 0.01$, vs. the control group, # represents $P < 0.05$, ## represents $P < 0.01$, vs. the DCM group.

Acupuncture reduces cardiac fibrosis and fibrosis-related gene expression in mice with diabetic cardiomyopathy

Masson's staining of the ventricles revealed that acupuncture at PC6+ST36 significantly decreased the degree of fibrosis in the ventricle, whereas the opposite trend was observed in the DCM group ($P < 0.05$, **Figure 4A**, **4B**). There were 510 genes expression significantly differed between the DCM and control groups and 622 genes expression significantly differed

between the acupuncture and DCM groups (see heatmap, **Figure 4C**). Some fibrosis-related genes were intuitively used to generate a heatmap (**Figure 4D**). The typical genes included *Col1a1*, *Col4a1*, *Col5a1*, *Col6a3*, *Apln*, and *Timp1*, which belong to the collagen fiber-forming family. Type I collagen α1 (COL1a1), also known as type alpha-1 collagen, is a protein encoded by the *Col1a1* gene. The expression result was verified at the protein level at the same time. Compared with that in the control group, the level of COL1a1 sharply increased in the DCM group, whereas acupuncture effectively reversed this increase (**Figure 4E**, **4F**).

Acupuncture inhibits cardiac apoptosis and autophagy in mice with diabetic cardiomyopathy

As reported in the literature, apoptosis and autophagy are dynamic during the development of diabetic cardiomyopathy [33]; thus, we detected apoptosis and autophagy levels via TUNEL staining and transmission electron microscopy, respectively. Compared with that in the control group, the average optical density of apoptotic cardiomyocytes sharply increased in the DCM group, whereas acupuncture effectively reduced it ($P < 0.05$, **Figure 5A**). The anti-apoptotic protein BCL2 displayed identical changes at the same time ($P < 0.05$, **Figure 5B**). Transmission electron microscopy revealed that the mitochondrial structure was damaged in the myocardium of mice with DCM and that the number and volume of lipid droplets increased (**Figure 5C**).

Acupuncture regulates the level of histone modification at the promoter region of Col1a1, which may affect its gene transcription during the development of diabetic cardiomyopathy with acupuncture intervention

Histone modification is an important form of epigenetic regulation that affects gene expression by altering the structure and state of chromatin. This modification can affect the activity of gene promoters and enhancers, which in turn affects transcription factor binding and RNA polymerase recruitment, thereby affecting gene transcription and expression. Type I collagen is the main component of the extracellular matrix (ECM) and the main extracellular substance deposited at the lesion site during organ fibrosis, which plays an important role in the development of diabetic cardiomyopathy [34]. Compared with those in the control group, both H3K4me1 and H3K27ace were more strongly associated with the promoter region of *Col1a1* than that in the DCM group and can promote gene expression [35]. Acupuncture treatment weakened this binding, which may reduce *Col1a1* gene expression (**Figure 6**).

Discussion

In animal research, acupuncture at ST36 (single acupoint) exerts a positive effect on multiple internal organs and is the most commonly used acupoint in both clinical and experimental studies related to type 2 diabetes. Many studies, including our previous studies, [8, 9] have verified these results. EA at ST36 combined with PC6, SP6, and BL23 alleviated pancreatic islet inflammation in rats with high-fat diet-induced insulin resistance. In addition, acupuncture ameliorates endothelial dysfunction via activation of the PI3K-Akt signalling pathway [36]. Our previous study revealed that EA treatment at Zusanli (ST36) and Neiting (ST44) causes clear weight loss in *Stat*5NKO mice by regulating abnormal lipid and glucose metabolism through the modulation of abnormal gene profiles in the hypothalamus and Epi-WAT [8]. Gong et al. verified that EA at ST36 reduces HFD-induced hepatic lipid accumulation in male Sprague-Dawley rats through the AMPK signalling pathway [7]. Firouzjaei et al. reported that acupuncture is an insulin sensitizer combined with metformin to improve insulin sensitivity, possibly by reducing body weight and inflammation and normalizing lipid metabolism and adipokines in type 2 diabetes patients. A series of acupoints, including ST36, were applied in their clinical study [19]. Our team also reported that EA can promote angiogenesis through H3K9 acetylation level at the *Vegf* gene after myocardial ischemia [23], as well as before ischemia - reperfusion injury, which alters the expression of numerous mRNAs associated with several pathways related to oxidative stress; cardiac muscle contraction; and gap junctions, vascular smooth muscle contraction, hypertrophy, NOD-like receptor, and P53 and B-cell receptor activation [37]. Thus, in our current research, PC6 and ST36 (both bilaterally) was selected to explore the potential effects of acupuncture on the progression of DCM.

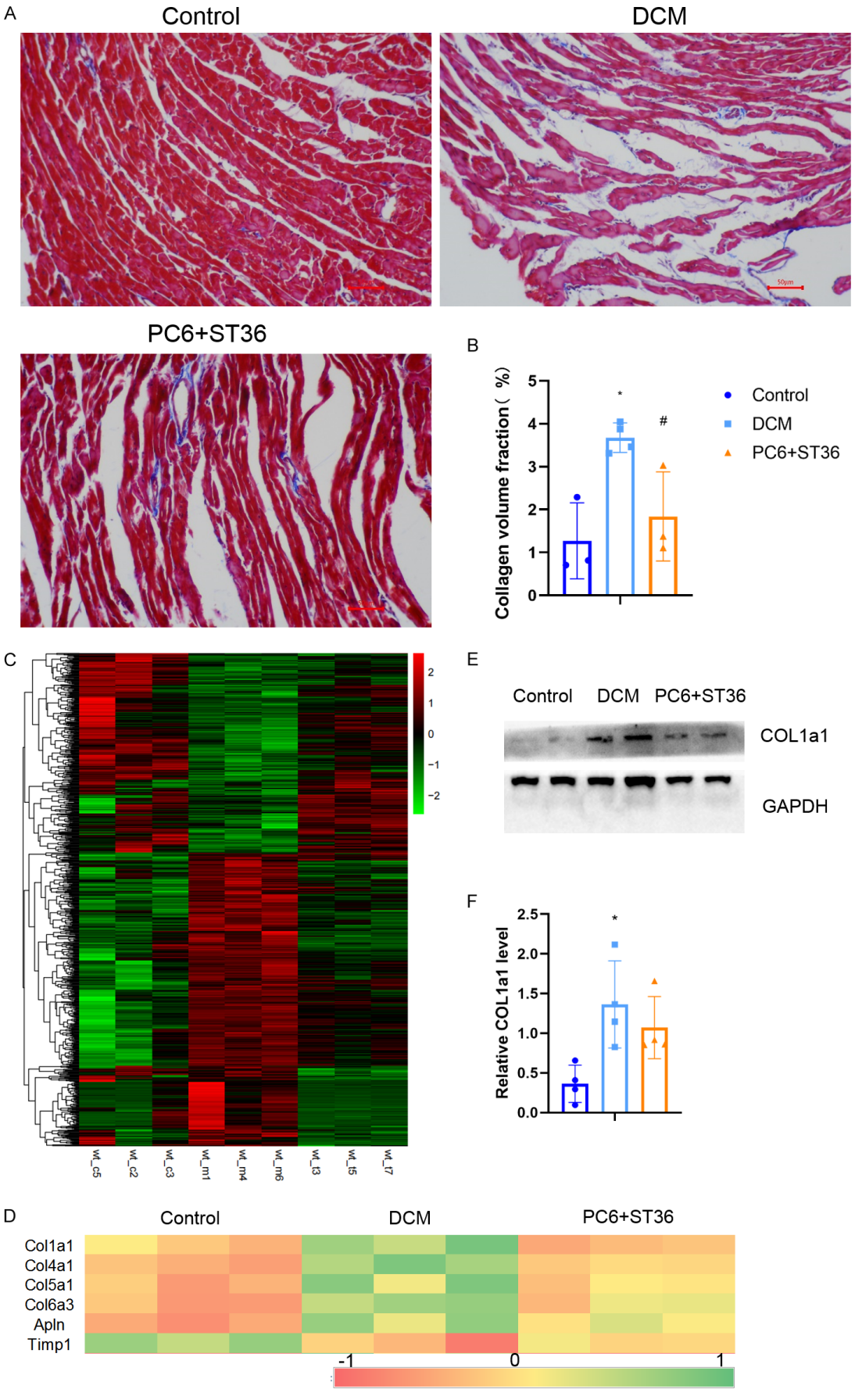
A
Control
DCM
PC6+ST36
B
Collagen volume fraction（%）
Control
DCM
PC6+ST36
C
E
Control
DCM
PC6+ST36
COL1a1
GAPDH
F
Relative COL1a1 level
D
Control
DCM
PC6+ST36
Col1a1
Col4a1
Col5a1
Col6a3
Apln
Timp1

Figure 4. Acupuncture reduces cardiac fibrosis and fibrosis-related gene expression in mice with diabetic cardiomyopathy. A. Tissue sections and fibrosis in the ventricle determined by calculating collagen deposition after Masson's trichrome staining in the control, DCM, and PC6+ST36 groups. Scale bar: 200 μm. B. Collagen deposition indices of the different groups; n=3-4 in each group. C. Heatmap of all the DEGs; a log2 (FC) > |±1| and $P < 0.05$ were used for analysis, n=3 in each group. D. Heatmap of collagen-related gene expression, n=3 in each group. E, F. Representative western blotting images of COL1α1 and analysis of heart tissues from the control, DCM, and PC6+ST36 groups, n=4 in each group, two independent sample experiments.

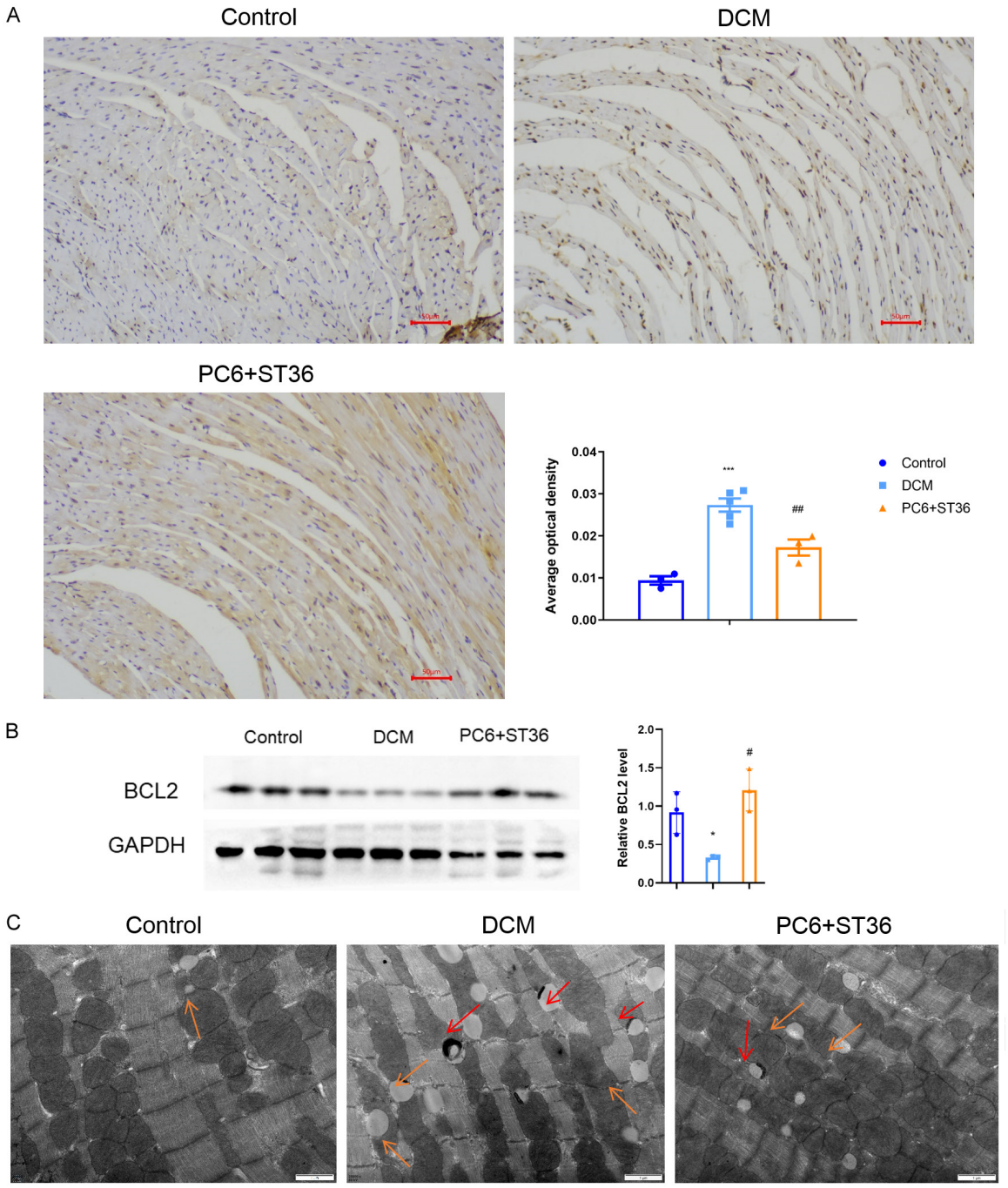

Figure 5. Acupuncture inhibits cardiac apoptosis and autophagy in mice with diabetic cardiomyopathy to some extent. A. Representative images of immunohistochemical staining for apoptosis and analysis of heart tissues from the control, DCM, and PC6+ST36 groups; n=3-5 in each group. Scale bar: 50 μm. B. Representative BCL2 immunohistochemical staining and analysis of heart tissues from the control, DCM, and PC6+ST36 groups; n=3 in each

group. C. Transmission electron microscopy. The myocardium of mice from the control group maintained continuous regular sarcomeres and constituted myofibrils, with mitochondria distributed between myofibrils that were structurally intact (yellow arrows represent fat droplets). The myofibrils of the myocardium in the mice in the DCM group were fragmented and disorganized, and the mitochondria were arranged in a disorganized manner with broken cristae and inner membranes that were swollen and vacuolated or ruptured (red arrows represent lysosomes involved in phagocytosis). The arrangement of the myocardial sarcomeres in the mice in the PC6+ST36 group was normal, with an intact mitochondrial structure and limited swelling and vacuoles. n=3 in each group. Scale bar: 1 μm.

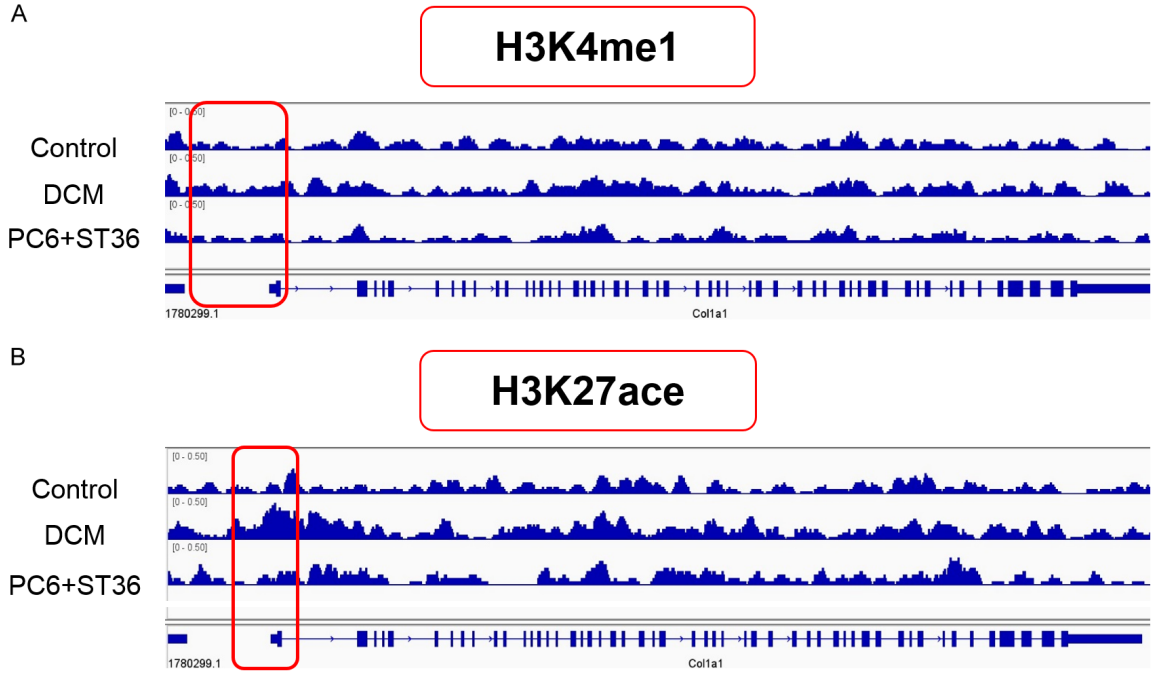

Figure 6. CUT&Tug analyses for the enrichment of methylated H3K4 and acetylated H3K27 on the *Col1a1* promoter region. For CUT&Tug analysis, chromatin was extracted from the hearts of each group and precipitated with antibodies against H3K4me1 and H3K27ace. The results were performed to amplify gene promoter regions and normalized with respect to input (the red box was used to mark promoter regions). A. H3K4me1 levels at the *Col1a1* promoter regions. B. H3K27ace levels at the *Col1a1* promoter regions. n=2 in each group.

In this study, we found that acupuncture can reduce fed glucose, improve HOMA-IR index. GTT and ITT displayed the result that mice in the acupuncture group company with enhanced insulin sensitivity. Abnormal lipid metabolism was also reversed at the same time. Both systolic and diastolic function were improved in mice with DCM. Cardiac fibrosis was also alleviated in the acupuncture group, accompanied by reduced expression of fibrosis-related genes. Moreover, acupuncture inhibited cardiac apoptosis in mice with DCM to some extent. All these results have been reported sporadically in other relevant studies, but we demonstrated these much more comprehensively here.

Gene expression depends on chromatin structure, which in turn relies on the epigenetic modification of histones. Hyperacetylated H3K27 or methylated H3K4 facilitates gene transcription [38]. Our team also demonstrated this protective role in mice with myocardial ischemic injury. We found that KMT2D attenuates angiogenesis by inhibiting the activation of VEGF-A transcription in the ischemic heart [24], which directly methylate H3K4, in turn binding to *Rasd1* GRE motifs in its enhancers and promoting its transcription in the presence of serum [25]. Genome-wide association analysis revealed changes in the lysine di-methylation levels of histone 3 lysine 4 and lysine 9 (H3K4 and H3K9) in human monocytes treated with high glucose, including interleukin 1 and interleukin 8 gene expression [39]. Gene expression of the long-term hyperglycemia-induced nuclear transcription factor NF-κB-p65 is closely associated with increased H3K4me1 and decreased

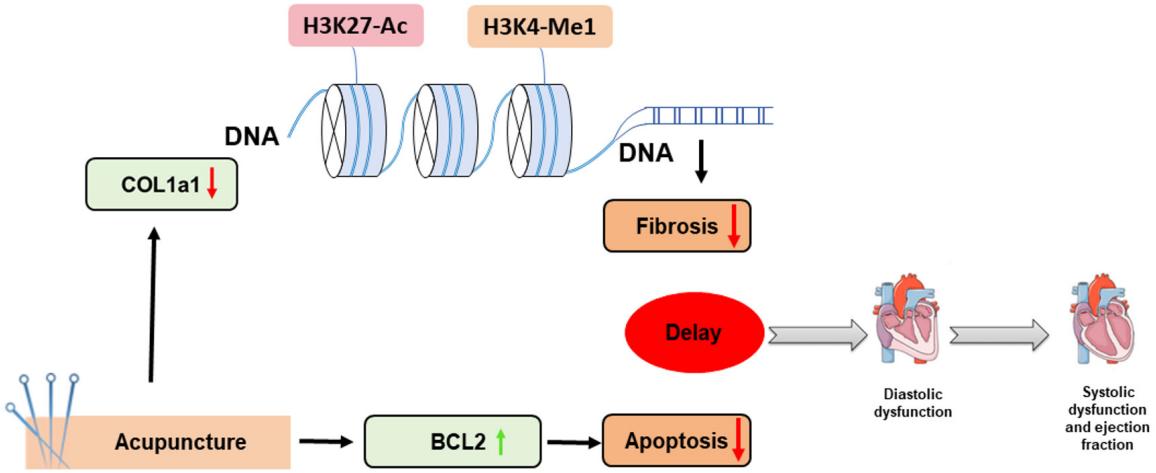

Figure 7. Graphical abstract of the mechanism of protective effect of acupuncture in mice with diabetic cardiomyopathy.

H3K9me2/me3 levels in patients with vascular complications of diabetes. Moreover, long-term hyperglycemia *in vivo* can cause cardiomyocyte apoptosis and autophagy, which exacerbate cardiomyocyte injury together with inflammation, thereby affecting heart systolic and diastolic function. Therefore, hyperglycemia-induced *Col1a1* gene expression is well known [40]. Here we demonstrated that both H3K4me1 and H3K27ace were strongly associated with the promoter region of *Col1a1* in the DCM group, which can promote gene expression and affect the development of fibrosis further. Acupuncture treatment weakens histone binding at *Col1a1* gene promoter, which may reduce *Col1a1* gene expression through different modification, thus alleviating fibrosis and delaying the development of diabetic cardiomyopathy.

Our results suggested that acupuncture at PC6 and ST36 is very effective in delaying DCM progression and gave some rudimentary mechanism for its role. Although our findings may guide future efforts to develop novel drugs useful for the treatment of diabetes patients, one limitation must be mentioned. That is we have not established a direct histone modification enzyme deletion animal model to verify the regulatory role of acupuncture in diabetic cardiomyopathy. Additionally, it remains unclear whether the beneficial effects of acupuncture are a direct result of histone modification modulation or secondary to improved glycemic control. Further research is necessary to delineate these mechanisms. Despite these limitations, our findings provide a foundation for future studies aimed at identifying novel therapeutic targets for the treatment of diabetic cardiomyopathy.

Conclusion

In this study, we demonstrated that acupuncture at Neiguan (PC6) and Zusanli (ST36) acupoints improves heart function in mice with diabetic cardiomyopathy through inhibiting cardiac apoptosis and fibrosis. These results are consistent with those of previous studies showing that acupuncture has multiple regulatory effects, including activating the nervous system, regulating the endocrine system, affecting the immune system, intervening in the autonomic nervous system, and regulating biological networks [41-43]. Here, we demonstrated that acupuncture at PC6 and ST36 could promote glycemic control and reduce diabetes-induced fibrosis to prevent the progression of DCM. The protective effect is likely related to the level of histone modification at the promoter region of fibrosis-related genes, which is a challenge for future studies (**Figure 7**, graphical abstract).

Acknowledgements

We wish to thank Prof. Cheng Peng and Dr. Chen Sun at the State Key Laboratory of Southwestern Chinese Medicine Resources, Chengdu University of Traditional Chinese Medicine, for their technical assistance. This

study was supported by the National Natural Science Foundation of China (No. 82105000), the Gusu Talent Program (No. 2023-013), the Sichuan International Science and Technology Innovation Cooperation Project (2023YFH-0013), the Jiangsu Double Innovation Doctor Program (No. JSSCBS20230519), the Suzhou Industrial Park Healthcare Talent Support Initiative (2024-32) and the Postdoctoral Research and Development Fund of West China Hospital, Sichuan University (No. 2020-HXBH049).

Disclosure of conflict of interest

None.

Abbreviations

ECG, Electrocardiogram; EF, Ejection fraction; FS, Fractional shortening; SV, Stroke volume; HR, Heart rate; Col1α, Collagen fiber 1α.

Address correspondence to: Dr. Bing-Mei Zhu, Regenerative Medicine Research Center, West China Hospital, Sichuan University, Keyuan Road 4, Gaopeng Street, Chengdu 610041, Sichuan, P. R. China. Tel: +86-28-85164069; Fax: +86-28-85164037; E-mail: zhubm64@hotmail.com

References

[1] Dillmann WH. Diabetic cardiomyopathy. Circ Res 2019; 124: 1160-1162.

[2] Jia G, Hill MA and Sowers JR. Diabetic cardiomyopathy: an update of mechanisms contributing to this clinical entity. Circ Res 2018; 122: 624-638.

[3] Filardi T, Ghinassi B, Di Baldassarre A, Tanzilli G, Morano S, Lenzi A, Basili S and Crescioli C. Cardiomyopathy associated with diabetes: the central role of the cardiomyocyte. Int J Mol Sci 2019; 20: 3299.

[4] Kowalska K, Wilczopolski P, Buławska D, Młynarska E, Rysz J and Franczyk B. The importance of SGLT-2 inhibitors as both the prevention and the treatment of diabetic cardiomyopathy. Antioxidants (Basel) 2022; 11: 2500.

[5] Pandey S, Mangmool S and Parichatikanond W. Multifaceted roles of GLP-1 and its analogs: a review on molecular mechanisms with a cardiotherapeutic perspective. Pharmaceuticals (Basel) 2023; 16: 836.

[6] Shapira MY, Appelbaum EY, Hirshberg B, Mizrahi Y, Bar-On H and Ziv E. A sustained, non-insulin related, hypoglycaemic effect of electroacupuncture in diabetic psammomys obesus. Diabetologia 2000; 43: 809-813.

[7] Gong M, Cao C, Chen F, Li Q, Bi X, Sun Y and Zhan Z. Electroacupuncture attenuates hepatic lipid accumulation via AMP-activated protein kinase (AMPK) activation in obese rats. Acupunct Med 2016; 34: 209-214.

[8] Fu SP, Hong H, Lu SF, Hu CJ, Xu HX, Li Q, Yu ML, Ou C, Meng JZ, Wang TL, Hennighausen L and Zhu BM. Genome-wide regulation of electroacupuncture on the neural Stat5-loss-induced obese mice. PLoS One 2017; 12: e181948.

[9] Shen W, Wang Y, Lu SF, Hong H, Fu S, He S, Li Q, Yue J, Xu B and Zhu BM. Acupuncture promotes white adipose tissue browning by inducing UCP1 expression on DIO mice. BMC Complement Altern Med 2014; 14: 501.

[10] Jing X, Ou C, Chen H, Wang T, Xu B, Lu S and Zhu BM. Electroacupuncture reduces weight gain induced by rosiglitazone through PPARγ and leptin receptor in CNS. Evid Based Complement Alternat Med 2016; 2016: 8098561.

[11] Cao B, Li R, Tian H, Ma Y, Hu X, Jia N and Wang Y. Effect on glycemia in rats with type 2 diabetes induced by streptozotocin: low-frequency electro-pulse needling stimulated Weiwanxiashu (EX-B 3) and Zusanli (ST 36). J Tradit Chin Med 2016; 36: 768-78.

[12] Ye Y, Birnbaum Y, Widen SG, Zhang Z, Zhu S, Bajaj M and Chen H. Acupuncture reduces hypertrophy and cardiac fibrosis, and improves heart function in mice with diabetic cardiomyopathy. Cardiovasc Drugs Ther 2020; 34: 835-848.

[13] Zhang L, Chen X, Wang H, Huang H, Li M, Yao L, Ma S, Zhong Z, Yang H and Wang H. "Adjusting internal organs and dredging channel" electroacupuncture ameliorates insulin resistance in type 2 diabetes mellitus by regulating the intestinal flora and inhibiting inflammation. Diabetes Metab Syndr Obes 2021; 14: 2595-2607.

[14] Wang H, Chen X, Chen C, Pan T, Li M, Yao L, Li X, Lu Q, Wang H and Wang Z. Electroacupuncture at lower He-Sea and Front-Mu acupoints ameliorates insulin resistance in type 2 diabetes mellitus by regulating the intestinal flora and gut barrier. Diabetes Metab Syndr Obes 2022; 15: 2265-2276.

[15] Liu Y, Sun X, Yuan M, Yu Z, Hou Q, Jia Z, Xu T and Xu B. Enhanced lipid metabolism reprogramming in CHF rats through IL-6-mediated cardiac glial cell modulation by digilanid C and electroacupuncture stimulation combination. Front Cell Dev Biol 2024; 12: 1424395.

[16] Martinez B and Peplow PV. Treatment of insulin resistance by acupuncture: a review of human and animal studies. Acupunct Med 2016; 34: 310-319.

[17] Meyer-Hamme G, Friedemann T, Greten HJ, Plaetke R, Gerloff C and Schroeder S. ACUDIN

- acupuncture and laser acupuncture for treatment of Diabetic peripheral Neuropathy: a randomized, placebo-controlled, partially double-blinded trial. BMC Neurol 2018; 18: 40.
[18] Danielli Miller N, Schiff E, Ben-Arye E, Singer J, Tsadok Perets T, Flaut S, Sahar N, Niv Y and Dickman R. Benefits of acupuncture for diabetic gastroparesis: a comparative preliminary study. Acupunct Med 2014; 32: 139-145.
[19] Firouzjaei A, Li GC, Wang N, Liu WX and Zhu BM. Comparative evaluation of the therapeutic effect of metformin monotherapy with metformin and acupuncture combined therapy on weight loss and insulin sensitivity in diabetic patients. Nutr Diabetes 2016; 6: e209.
[20] Wang SY, Deng CX, Huang YN, Tian MX, Zhuang SY, Deng YF, Xu B and Xu TC. Electroacupuncture in glycemic control: transitioning from clinical controversies to potential basic research. World J Diabetes 2025; 16: 112580.
[21] Kan RL, Chen J and Sallam T. Crosstalk between epitranscriptomic and epigenetic mechanisms in gene regulation. Trends Genet 2022; 38: 182-193.
[22] Heinz S, Romanoski CE, Benner C and Glass CK. The selection and function of cell type-specific enhancers. Nat Rev Mol Cell Biol 2015; 16: 144-154.
[23] Fu SP, He SY, Xu B, Hu CJ, Lu SF, Shen WX, Huang Y, Hong H, Li Q, Wang N, Liu XL, Liang F and Zhu BM. Acupuncture promotes angiogenesis after myocardial ischemia through H3K9 acetylation regulation at *Vegf* gene. PLoS One 2014; 9: e94604.
[24] Meng XM, Liu SB, Deng T, Li DY, You L, Hong H, Feng QP and Zhu BM. Loss of histone methyltransferase KMT2D attenuates angiogenesis in the ischemic heart by inhibiting the transcriptional activation of VEGF-A. J Cardiovasc Transl Res 2023; 16: 1032-1049.
[25] Liu SB, Meng XM, Li YM, Wang JM, Guo HH, Wang C and Zhu BM. Histone methyltransferase KMT2D contributes to the protection of myocardial ischemic injury. Front Cell Dev Biol 2022; 10: 946484.
[26] Reed MJ, Meszaros K, Entes LJ, Claypool MD, Pinkett JG, Gadbois TM and Reaven GM. A new rat model of type 2 diabetes: the fat-fed, streptozotocin-treated rat. Metabolism 2000; 49: 1390-1394.
[27] Hong H, Cao X, Deng T, Meng XM, Li YM, Zhu LJ, Lv J, Li X, Yu SG and Zhu BM. Acupuncture at Neiguan suppresses PVCs occurring post-myocardial infarction by alleviating inflammation and fibrosis. Chin Med 2022; 17: 52.
[28] Hong H, Cao X, Meng XM, Pang QY, Zhu LJ, Yu SG and Zhu BM. Comparative study of different acupoints for treating acute myocardial ischemia in mice. J Cardiovasc Transl Res 2023; 16: 644-661.
[29] Shi Y, Liao Y, Liu Q, Ni Z, Zhang Z, Shi M, Li P, Li H and Rao Y. BRD4-targeting PROTAC as a unique tool to study biomolecular condensates. Cell Discov 2023; 9: 47.
[30] Zhu BM, Kang K, Yu JH, Chen W, Smith HE, Lee D, Sun HW, Wei L and Hennighausen L. Genome-wide analyses reveal the extent of opportunistic STAT5 binding that does not yield transcriptional activation of neighboring genes. Nucleic Acids Res 2012; 40: 4461-4472.
[31] Ramírez F, Ryan DP, Grüning B, Bhardwaj V, Kilpert F, Richter AS, Heyne S, Dündar F and Manke T. deepTools2: a next generation web server for deep-sequencing data analysis. Nucleic Acids Res 2016; 44: W160-W165.
[32] Robinson JT, Thorvaldsdóttir H, Winckler W, Guttman M, Lander ES, Getz G and Mesirov JP. Integrative genomics viewer. Nat Biotechnol 2011; 29: 24-26.
[33] Liu C, Yao Q, Hu T, Cai Z, Xie Q, Zhao J, Yuan Y, Ni J and Wu QQ. Cathepsin B deteriorates diabetic cardiomyopathy induced by streptozotocin via promoting NLRP3-mediated pyroptosis. Mol Ther Nucleic Acids 2022; 30: 198-207.
[34] Dai X, Yang F, Chen D, Yang L, Dong Z, Chen C and Xiao J. The role of fibromodulin in myocardial fibrosis in a diabetic cardiomyopathy rat model. FEBS Open Bio 2025; 15: 436-446.
[35] Chen W, Wang F, Yu X, Qi J, Dong H, Cui B, Zhang Q, Wu Y, An J, Ni N, Liu C, Han Y, Zhang S, Schmitt CA, Deng J, Yu Y and Du J. LncRNA MIR31HG fosters stemness malignant features of non-small cell lung cancer via H3K4me1- and H3K27Ace-mediated GLI2 expression. Oncogene 2024; 43: 1328-1340.
[36] Lan D, Xu N, Sun J, Li Z, Liao R, Zhang H, Liang X and Yi W. Electroacupuncture mitigates endothelial dysfunction via effects on the PI3K/Akt signalling pathway in high fat diet-induced insulin-resistant rats. Acupunct Med 2018; 36: 162-169.
[37] Huang Y, Lu SF, Hu CJ, Fu SP, Shen WX, Liu WX, Li Q, Wang N, He SY, Liang FR and Zhu BM. Electro-acupuncture at Neiguan pretreatment alters genome-wide gene expressions and protects rat myocardium against ischemia-reperfusion. Molecules 2014; 19: 16158-16178.
[38] Hu Y, He Z, Li Z, Wang Y, Wu N, Sun H, Zhou Z, Hu Q and Cong X. Lactylation: the novel histone modification influence on gene expression, protein function, and disease. Clin Epigenetics 2024; 16: 72.
[39] Brasacchio D, Okabe J, Tikellis C, Balcerczyk A, George P, Baker EK, Calkin AC, Brownlee M, Cooper ME and El-Osta A. Hyperglycemia induces a dynamic cooperativity of histone

methylase and demethylase enzymes associated with gene-activating epigenetic marks that coexist on the lysine tail. Diabetes 2009; 58: 1229-1236.

[40] Liu Z, Hayashi H, Matsumura K, Ogata Y, Sato H, Shiraishi Y, Uemura N, Miyata T, Higashi T, Nakagawa S, Mima K, Imai K and Baba H. Hyperglycaemia induces metabolic reprogramming into a glycolytic phenotype and promotes epithelial-mesenchymal transitions via YAP/TAZ-Hedgehog signalling axis in pancreatic cancer. Br J Cancer 2023; 128: 844-856.

[41] Tian M, Sun W, Mao Y, Zhang Y, Liu H and Tang Y. Mechanistic study of acupuncture on the pterygopalatine ganglion to improve allergic rhinitis: analysis of multi-target effects based on bioinformatics/network topology strategie. Brief Bioinform 2024; 25: bbae287.

[42] Zheng H, Wang G, Liu M and Cheng H. Traditional Chinese medicine inhibits PD-1/PD-L1 axis to sensitize cancer immunotherapy: a literature review. Front Oncol 2023; 13: 1168226.

[43] Guo J, Guo J, Rao X, Zhang R, Li Q, Zhang K, Ma S, Zhao J and Ji C. Exploring the pathogenesis of insomnia and acupuncture intervention strategies based on the microbiota-gut-brain axis. Front Microbiol 2024; 15: 1456848.

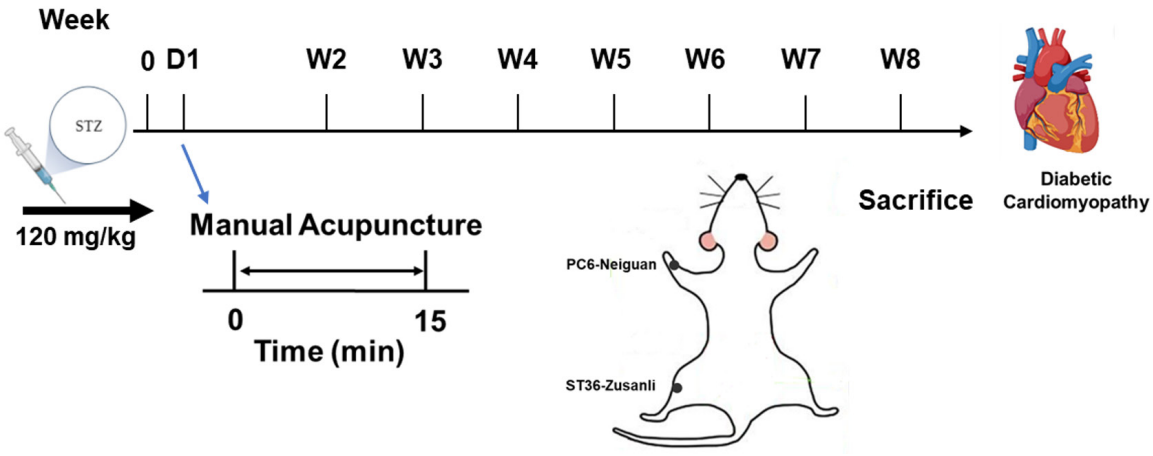

Supplementary Figure 1. Acupoint location map and our experimental flow chart.